Pergamon

Adv. Space Res. Vol. 21, No. 10, pp. 1383–1391, 1998

Printed in Great Britain
0273-1177/98 $19.00 + 0.00

PII: S0273-1177(97)00746-1

DISTRIBUTION AND SEASONAL VARIATION OF CFCS IN THE STRATOSPHERE: COMPARISON OF SATELLITE GLOBAL DATA AND A 2-D MODEL

A. E. Roche*, R. W. Nightingale*, J. B. Kumer*, J. L. Mergenthaler*, C. H. Jackman** and E. L. Fleming***

** Lockheed Martin Palo Alto Research Laboratory, Palo Alto, CA 94304, USA*
*** NASA/Goddard Space Flight Center, Greenbelt, MD 20771, U.S.A.*
**** Applied Research Corporation, Landover, MD 20785, U.S.A.*

ABSTRACT

The Cryogenic Limb Array Etalon Spectrometer (CLAES) on the NASA Upper Atmosphere Research Satellite obtained global distributions of CF_2Cl_2 and $CFCl_3$ in the stratosphere between October 1991 and May 1993. This paper discusses the seasonal and interannual behavior of a number of prominent dynamical features observed in the zonal mean fields for both gases over the period January 1992 through February 1993 and compares these features with a two-dimensional model. The CFC fields are shown to exhibit many of the same seasonally variant features seen in other conserved tracer fields. These include a semiannual oscillation signature in the tropical upper-level mixing ratios; the development of a double-peaked tropical structure near the vernal equinox and its weakening, or absence, at the autumnal equinox; steep descent at winter high latitudes in both hemispheres with an associated midlatitude surf zone, which is stronger and more sustained in the southern hemisphere; and sharp subtropical gradients in the mixing ratio isopleths in the northern winter hemisphere. Distinct interannual variability is also observed in the CF_2Cl_2 morphology, particularly for the northern hemisphere for the periods January-February 1992 and 1993. Other than this latter feature, the two-dimensional model is generally found to reproduce the observed behavior, although usually with weaker manifestation than seen in the data, especially in regard to the double-peaked equinoctial structure.

INTRODUCTION

CF_2Cl_2 and $CFCl_3$ with global mean tropospheric mixing ratios in 1995 of approximately 530 and 270 parts per trillion volume (pptv), respectively, are the most abundant of the industrially produced organic chlorine compounds (Montzka et al., 1996). In the stratosphere UV photolysis of these and other organic chlorine compounds results in the production of free chlorine enabling the destruction of ozone through various catalytic mechanisms. CF_2Cl_2 and $CFCl_3$ together currently contribute more than half of the 3.5 ppbv total mean chlorine in the stratosphere (Zander et al., 1996). Therefore, they are of major importance in the understanding of global ozone loss and in the prediction of the response of the stratosphere to reductions in CFC emissions. These CFCs are also very useful as tracers of stratospheric air motions, especially in the low and mid stratosphere, either alone, or in concert with other frequently used tracers, such as N_2O and CH_4. In this paper we will concentrate mainly on this latter aspect, i.e., the use of CFC global field data to study large-scale features in stratospheric morphology and seasonal trends in such features.

CF_2Cl_2 and $CFCl_3$ were first detected in the stratosphere in 1968 by balloon-borne infrared solar occultation spectrometers (Murcray et al., 1975). Concentrations of these and other halocarbons have since been widely measured from balloon, airborne, and shuttle-based instruments (see Nightingale et al. (1996) and references therein). The first seasonal-cycle near-global measurements of CF_2Cl_2 and $CFCl_3$ were acquired by the Cryogenic Limb Array Etalon Spectrometer (CLAES) on the NASA Upper Atmosphere Research Satellite (UARS) over the period October 1991 to May 1993 (Roche et al., 1993; Nightingale et al., 1996). The Nightingale et al. paper discusses validation of CLAES CF_2Cl_2 data through correlative data comparisons and selected comparisons with a two-dimensional (2-D) model developed by the Lawrence Livermore National Laboratory (LLNL). In this paper we discuss the detailed seasonal and interannual global morphology of the altitude-latitude distributions of CF_2Cl_2, and for the first time of $CFCl_3$, as revealed by the CLAES measurements over the annual cycle January 1992 through February 1993. These data, along with other UARS tracer data, including N_2O and CH_4 from CLAES (Roche et al., 1996) and ISAMS (Remedios et al., 1996), and CH_4 from HALOE (Park et al., 1996), reveal in much greater detail many of the same characteristic features first observed in the NIMBUS-7 SAMS N_2O data (Jones and Pyle, 1984). Because of their more extended geographical coverage (especially involving high-latitude winter/spring situations), the CLAES data also reveal a number of new features not seen, or only weakly observed, in the SAMS data. To gain insight into the observed morphology and seasonal trends we compare the CLAES data fields with a 2-D chemical-transport model developed by the NASA Goddard Space Flight Center (GSFC).

CLAES DATA CHARACTERISTICS

CLAES is a limb viewing instrument deriving mixing ratio profiles of CF_2Cl_2, $CFCl_3$, nine other gases, temperature, and aerosol extinction coefficients from the measurement of infrared spectral radiances between about 15 and 60 km (Roche et al., 1993). Data were acquired simultaneously at 20 tangent altitudes nominally between 10 and 60 km, with 2.5 km vertical spacing. Measurement repeat time was 65 s corresponding to a horizontal grid size of about 500 km. The plane of the UARS 57° inclination orbit processes ~ 5° per day relative to the sun, and the spacecraft is yawed 180° approximately every 36 days. CLAES thus obtained alternating latitude coverage, either 34°N to 80°S, or 34°S to 80°N, depending on the UARS flight direction; coverage was continuous in the overlap band between 34°N and 34°S. The instrument telescope aperture door was closed for approximately 5 days around each yaw period for calibration and thermal protection purposes, and was closed an additional 1–2 days halfway between yaws for further calibration.

The general approach to the retrieval of geophysical data from the measured spectral radiances for version 7 (V7) of the data processing software is described in Kumer et al. (1996). Specifics of the retrieval of CF_2Cl_2 mixing ratios (from radiance emission near 922 cm^{-1}) are provided in Nightingale et al. (1996), who also discuss CF_2Cl_2 error estimation, data validation, and data quality. For the several-day zonal averages used in the current paper, the CF_2Cl_2 random error is at most 3 to 1.7 pptv, or < 4%, to as high as 3 mb in the tropics. CF_2Cl_2 systematic errors are in the range 14 to 22% between 46 and 5 mb. $CFCl_3$ is more susceptible to interference from other quasi-continuum emitters, especially polar stratospheric clouds (PSCs). The $CFCl_3$ data presented here, which were processed with an interim version 8 algorithm (V8), have been deliberately selected for periods of low PSC activity, and they have to date been subjected to far less intensive validation than that for CF_2Cl_2. The zonal mean random and systematic errors for the limited amount of $CFCl_3$ V8 data shown are likely to be at least twice those for CF_2Cl_2.

Zonal Mean Altitude-Latitude Cross Sections

CF_2Cl_2 Data Fields. The global morphology and seasonal behavior of CF_2Cl_2 are illustrated in the series of zonal mean cross sections presented in Figure 1. These cross sections were constructed by averaging 4–5 days of zonal mean altitude profiles on either side of spacecraft yaws between January 1992 and February 1993 and then combining the resulting north- and south-looking cross sections to provide pseudo 80°N to 80°S cross sections. This process gives a good instantaneous representation of the global morphology of the CF_2Cl_2 fields, since only 4–6 days separate the adjacent north and south looks. The combination of the separate cross sections is done only in the regions between 32°S and 32°N, which should be dynamically quiescent over this time period. The July data extend only to 65°S and the August data to 70°S because very dense PSCs, poleward of these latitudes during particularly cold periods in July and August, cause large retrieval errors in the V7 algorithm.

The overall morphology is characterized by upwelling in equatorial regions and movement poleward and downward in both hemispheres. The isopleths typically exhibit sharp latitudinal gradients in the extratropics near 20°. The seasonal behavior can be seen by examining the transition from the period close to the northern winter solstice

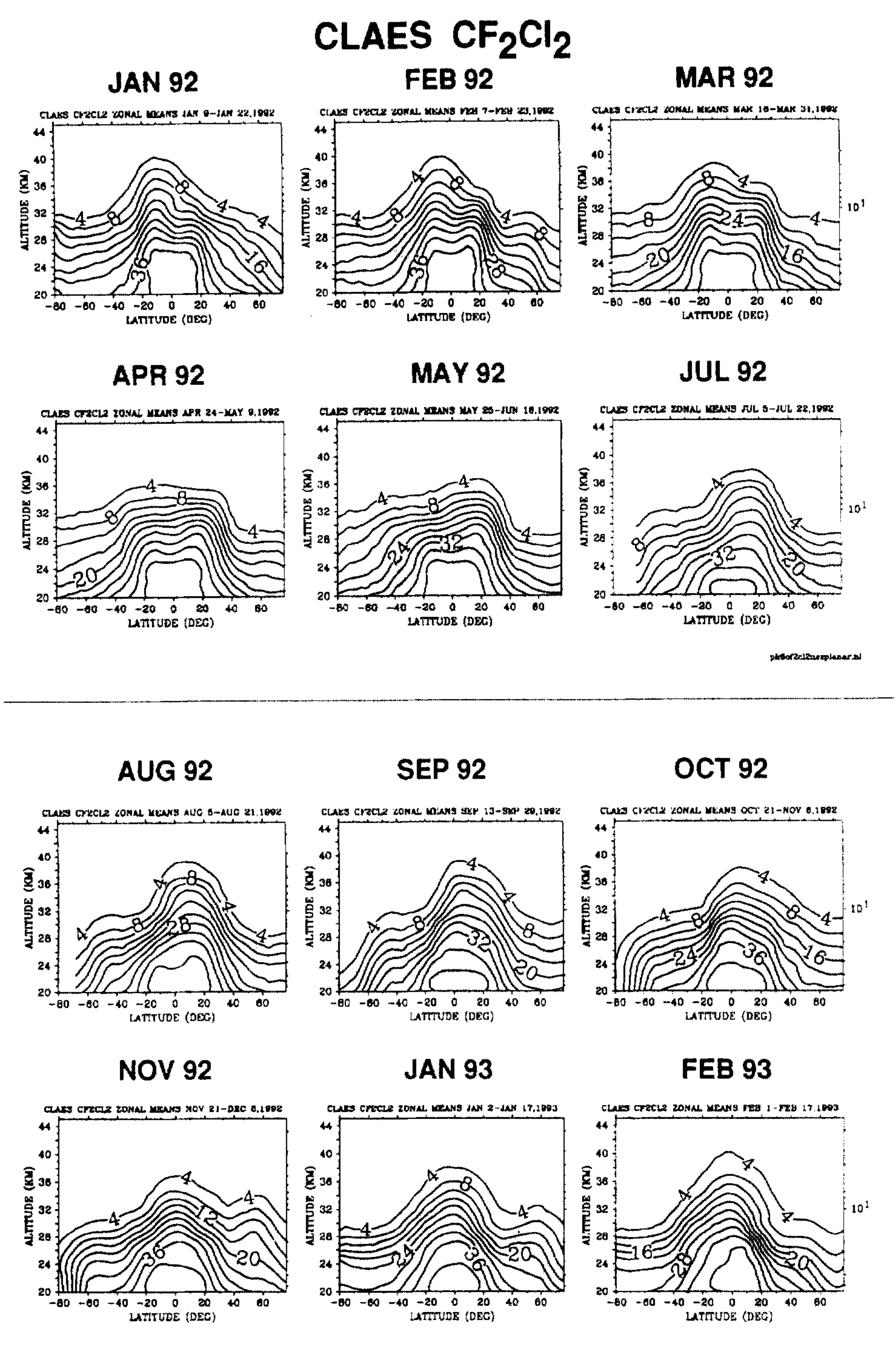

Fig. 1. CLAES CF_2Cl_2 zonal mean latitude-altitude mixing ratio cross sections. Each panel represents a combination of 5-day zonal averages on either side of a spacecraft yaw. Indicated contour numbers have units of 10 parts per trillion volume (i.e., exponent of 10^{-11}).

(January 1992) through the vernal equinox (March 1992) to the period near the summer solstice (July 1992). As Figure 1 shows, the isopleths tend to "lean" towards the summer hemisphere, with the isopleth bulge centered between 10° and 20°S, and they show nearly horizontal behavior from about 50° to 80°S in the summer hemisphere. By contrast in the winter hemisphere the isopleths show a steep downward gradient from 50° to 80°N associated with the northern winter vortex. In February/March in the northern hemisphere a region of quasi-horizontal isopleths develops from mid latitudes to about 60°N, near the edge of the arctic polar vortex. This is the so-called "surf zone," which is discussed further below.

By the March/April northern spring period the isopleths show a more symmetric shape with a double-peaked structure centered about the equator. More horizontal gradients are present from mid to high latitudes in both hemispheres, as the arctic vortex has dissipated and the southern vortex has not yet formed in any strength. By July 1992 a near-mirror image of the January 1992 structure has been established, with the isopleths now leaning towards the northern (summer) hemisphere and exhibiting horizontal behavior towards high northern latitudes. In the winter (southern) hemisphere the isopleths exhibit a distinct midlatitude surf zone region and steep downward gradients poleward of about 50°S with especially strong descent from 60° to 80°S, reflecting the presence of the very cold Antarctic winter vortex. We note again the steep gradients/sharp edges in the northern hemisphere winter fields in the subtropics.

There are some notable differences in the second half of the year as the seasons progress towards the next solstice period. Unlike the 1992 northern hemisphere spring, where the isopleth gradients at high latitudes have noticeably flattened by March 16, in the southern hemisphere steep gradients are observed as late as November 21 poleward of ~60°S, reflecting the influence of a much longer-lived polar vortex. Although the isopleth equatorial bulge structure moves back towards the summer hemisphere, the double-peaked structure is not evident in the southern spring September-October period. Finally, in comparing January 1992 with January 1993, although the southern hemisphere structures are quite similar, the northern hemisphere fields in 1993 show a pronounced surf zone region between ~40° and 60°N not seen in the 1992 January fields.

<u>$CFCl_3$ Data Fields.</u> Figure 2 shows selected zonal mean cross sections for $CFCl_3$, juxtaposed with CF_2Cl_2 panels from Figure 1 to facilitate direct comparison. These $CFCl_3$ fields show similar morphology and seasonal trends to the CF_2Cl_2 data. The movement of the isopleth maximum to follow the summer hemisphere is clearly seen in comparison between the January and September cross sections; a weaker but still evident double-peaked structure is visible in March; and the steep gradients in the winter/spring high latitudes are evident in the January (northern winter) and September (southern spring) data, in addition to the appearance of surf zone features in September and November.

<u>Discussion of CLAES CFC Data Fields</u>

<u>Winter High-Latitude Features.</u> These CFC measurements, along with CLAES and ISAMS N_2O and CH_4, are the first such data fields to have been acquired throughout the polar night winter and spring periods, especially in the Antarctic. They show clearly that these periods, especially in the southern hemisphere, are characterized by steep descent within and at the edges of the polar vortices between about 60 and 8 mb, the upper-altitude limit of the CF_2Cl_2 extratropical measurement range. CLAES and HALOE CH_4 data, which can be measured to much higher altitudes, show this descent to extend to as high as 0.5 mb (Roche et al., 1996; Park et al., 1996).

<u>Double-Peaked Structure.</u> The tendency for the upper level bulge in the CF_2Cl_2 fields to "follow" the summer hemisphere and the development of an equatorial double-peaked structure in the northern spring months were originally observed in the SAMS N_2O data and are thought to be associated with the semiannual oscillation (SAO) in the upper stratospheric equatorial winds (Gray and Pyle, 1987; Choi and Holton 1991). The absence of a double-peaked structure in the CLAES CFC fields in the southern spring was also noted in the SAMS data with the suggestion that it reflects differences in planetary wave activity in the two hemispheres (Holton and Choi, 1988). CLAES N_2O fields also show a weaker effect near the autumnal equinox (Randel et al., 1994).

<u>Surf Zone.</u> The formation of the surf zone, which is a persistent feature of the CFC fields equatorward of the polar vortices during the winter months, is a consequence of planetary wave breaking and isentropic mixing and was first

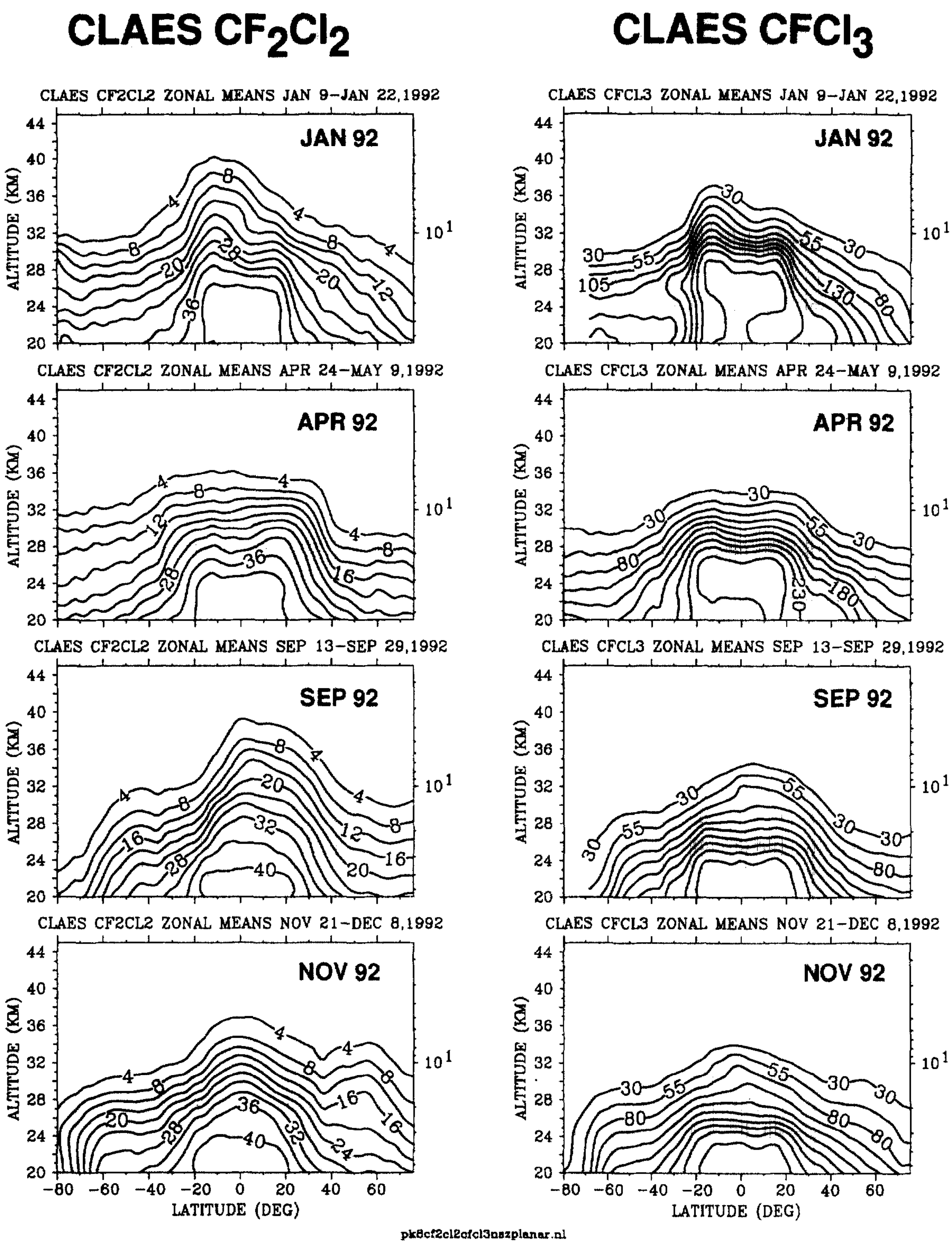

Fig. 2. CLAES CF_2Cl_2 and $CFCl_3$ zonal mean latitude-altitude mixing ratio cross sections for selected periods, constructed in the same manner as Figure 1. Contour units and intervals are as in Figure 1.

identified in potential vorticity fields by McIntyre and Palmer (1983). In addition to the CFC data shown here, surf zones are also clearly evident in CLAES N_2O and CH_4 fields (Randel et al., 1994; Roche et al., 1996).

Subtropical Barrier. The sharp edges in the CFC fields in the subtropics, especially in the northern hemisphere winter months, have also been observed in aerosol distributions (Grant et al., 1996; Mergenthaler et al., 1995) and in CLAES N_2O fields (Randel et al., 1993). It has been suggested that these sharp edges imply a barrier to mixing outside the extratropics (Waugh, 1996; Plumb , 1996; Minschwaner et al., 1996; Volk et al., 1996).

Comparison of CLAES CFC Fields with a 2-D Model.

A variety of 2-D models have been developed in recent years that attempt to reproduce the major features of observed stratospheric circulation and structure. For example, N_2O models by both Garcia et al. (1992) and Randel et al. (1994), reproduce with some success the winter hemisphere features of a midlatitude surf zone and steep descent within the polar vortex, when planetary and gravity wave formulations are included. However, both have difficulty with the SAO in the tropical upper stratosphere and the associated double-peaked structure observed near the vernal equinox, a difficulty encountered in earlier analysis of SAMS N_2O data (Choi and Holton, 1991). Nightingale et al. (1996) presented limited comparisons between CLAES CF_2Cl_2 data and the LLNL 2-D model for March and September 1992. In this paper, for detailed comparisons over the whole annual cycle, we chose the recently upgraded GSFC 2-D model.

GSFC 2-D Model. This model is described in detail in Jackman et al. (1996) and Considine et al. (1994). The model domain is from the surface to 90 km with ~ 2 km vertical resolution and from 85°S to 85°N with 10° latitude resolution. It incorporates 57 species, including the O_x, NO_x, HO_x, Cl_x, and Br_x families. Heterogeneous reactions on sulfate aerosols and PSCs are included. The model CF_2Cl_2 mixing ratios contain an annual increase based on source gas variations from WMO-37 (1995). The model has a fixed transport with self-consistent winds and eddy diffusion, and the transport is computed off-line and is uncoupled from constituent changes. Forcing from planetary and gravity waves is included. Figure 3 shows model zonal mean cross sections for CF_2Cl_2 for each month of the year using identical pressure and latitudinal scales to those for the CLAES data in Figure 1. Figure 4 shows the March model run with extended altitude coverage to emphasize the upper level contours. Overall, as Figure 3 demonstrates, the model shows good quantitative and qualitative agreement with the data fields, capturing most of the major morphological and seasonally varying features. The migration of the upper level isopleths across the equator from the southern summer hemisphere to the northern summer hemisphere is quite evident in comparing the January and July/August panels. Although not as strong as in the data, the descent of the isopleths near winter high latitudes is evident in the northern hemisphere in January and in the southern hemisphere in the August/September period. The development of a surf-zone feature is evident in September and October.

The success of the model in capturing these latter features is likely due to the inclusion of a planetary and gravity wave forcing formulation, as noted at the beginning of this section, although the tendency of the model to produce weaker effects than those seen in the data suggests that the forcing may not be sufficiently strong. This may be especially true for the southern hemisphere spring period when the model only weakly sustains the very steep isopleth gradients poleward of 60°S evident in the data in October and November. The model does show some indication of steep gradients in the subtropics in the northern winter/spring months (December–March). A disagreement between the data fields and model is evident in the absence of a double-peaked structure in the model near the vernal equinox, at and below the altitudes of the 40 pptv contour. The model, however, does show evidence for such a feature in the 15 pptv and higher altitude contours for March (Figure 4); and it is also seen at the higher altitudes in April (not shown). Difficulty in reproducing the double-peaked structure has been a common deficiency with 2-D models as noted above. Randel et al. (1994) suggest that this is due to weak gravity wave driving in their model, which results in a weakened downward velocity in the tropical upper stratosphere during the westerly (equinox) phase of the SAO. Choi and Holton (1991) found that to reproduce the double-peaked structure in their 2-D model they had to modify the meridional circulation by doubling the climatological values associated with the SAO wind and temperature fields. They conclude that the diabatic circulation must be considerably stronger than implied by standard climatologies. The appearance of the feature in the GSFC model only at the higher altitudes and in a relatively weak amplitude suggests that a somewhat similar situation may prevail for this model, but the success in reproducing the feature in any form is encouraging.

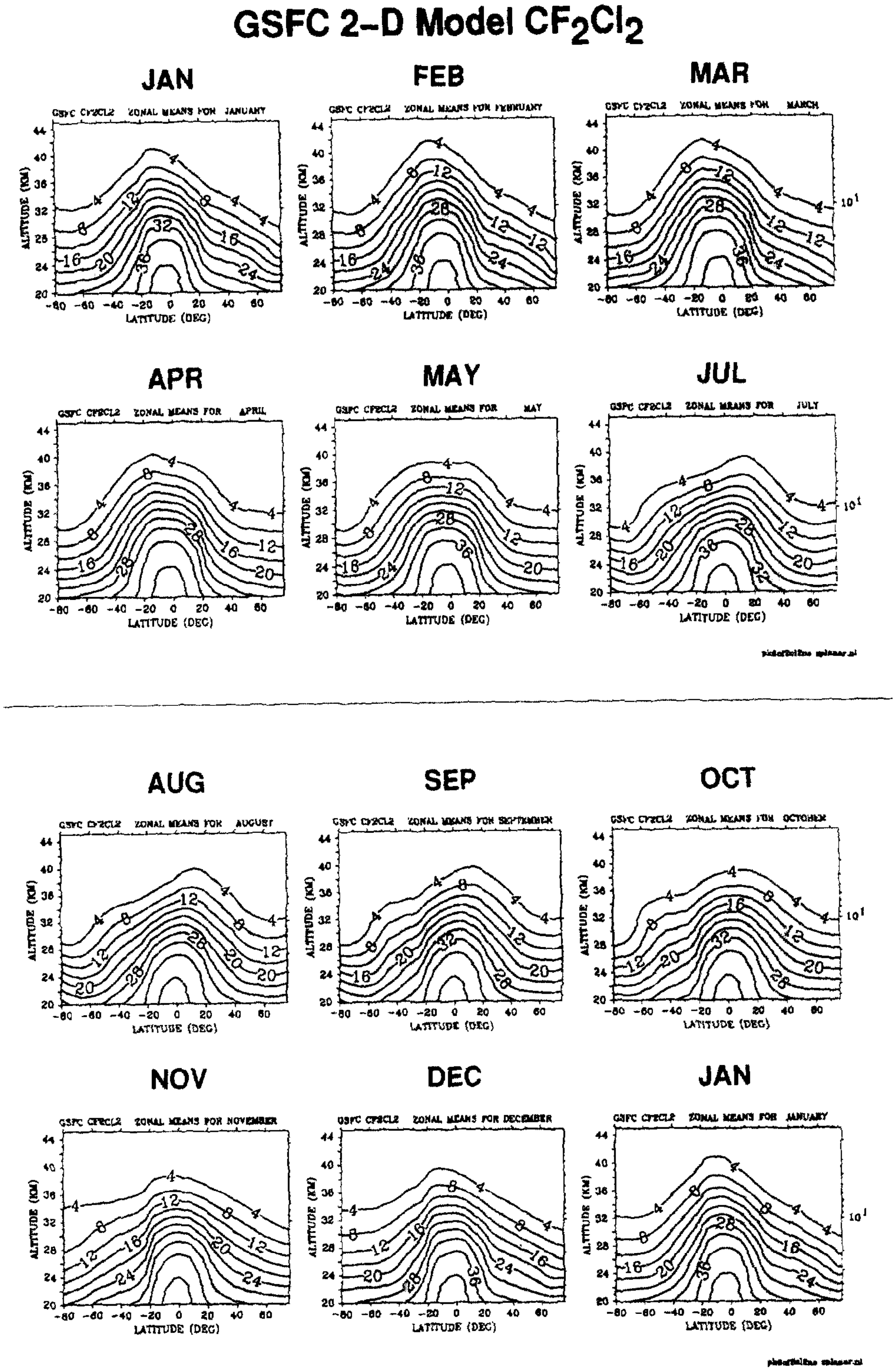

Fig. 3. GSFC model monthly zonal mean latitude-altitude mixing ratio cross sections. Scales are identical to those used in Figure 1.

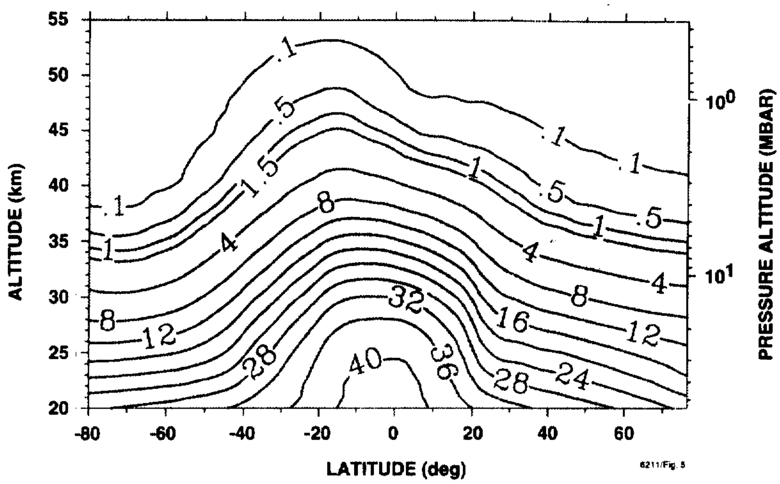

Fig. 4. GSFC model CF_2Cl_2 results for March extended to high altitudes. Units are as in Figure 1.

SUMMARY

The CLAES CF_2Cl_2 and $CFCl_3$ zonal mean data fields display many of the same seasonally variant dynamical features previously observed in other conserved tracers, including N_2O and CH_4. The CLAES zonal mean CFC data have an upper altitude measurement limit of about 3 mb, considerably lower than that for either N_2O (1 mb) or CH_4 (0.5 mb). Nevertheless, the 3.2 mb CFC fields show the same SAO signature as that seen in the upper level N_2O/CH_4 fields, including the tendency of the isopleth bulge to follow the summer hemisphere and the appearance of double-peaked structure about the equator near the vernal equinox. The CFC fields confirm the development of steep descending gradients in the isopleths at high latitudes in the winter/spring hemispheres observed in other tracers, especially in the southern hemisphere. They also show that this high-latitude descent feature and a distinct midlatitude surf zone on the equatorward side of the polar vortex develop as early as July 1992 and are maintained through early November 1992. The CFC fields also develop steep subtropical gradients in the northern hemisphere winter months, similar to other tracers and to the Pinatubo sulfate aerosol cloud. The CF_2Cl_2 zonal mean mixing ratios are in overall good agreement with the modeled values. Seasonal variations, descent of air near and inside the polar vortices and the appearance of an associated surf zone are reproduced in the GSFC 2-D model, although not as strongly as in the data fields, suggesting that planetary and gravity wave forcing formulation in the model is mechanistically correct but not strong enough. The double-peaked structure near the northern spring equinox is reproduced by the GSFC model only at the higher altitudes and also with fairly weak amplitude. The appearance of a double-peaked type structure in the model represents an advance over previous efforts, although the low amplitudes would suggest that the climatological input to the meridional circulation in the model still does not adequately represent the strength of the actual diabatic circulation.

ACKNOWLEDGMENTS

We wish to acknowledge the invaluable contributions of our Lockheed Martin colleagues John Potter, Gary Ely, and Frank Zele to the processing, analysis, and display of the data shown in this paper, and to our colleagues at NCAR, John Gille, Paul Bailey, and Steven Massie, for their contribution to data processing, validation, and analysis. This work was supported at Lockheed Martin under NASA contract NAS5-27752.

REFERENCES

Choi, W. K., and J. R. Holton, Transport of N_2O in the stratosphere related to the equatorial semiannual oscillation, *J. Geophys. Res.*, 96, 22543–22557, 1991.

Considine, D. B., A. R. Douglass and C. H. Jackman, Effects of a polar stratospheric cloud parameterization on ozone depletion due to stratospheric aircraft in a two-dimensional model, *J. Geophys. Res.*, 99, 18879–18894, 1994.

Garcia, R. R., F. Stordal, S. Solomon, and J. T. Kiehl, A new numerical model of the middle atmosphere, 1: Dynamics and transport of tropospheric trace species, *J. Geophys. Res.*, 97, 12967–12991, 1992.

Grant W. B., E. V. Browell, C. S. Long, L. L. Strowe, R. G. Grainger, and A. Lambert, Use of volcanic aerosols to study the tropical stratosphere reservoir, *J. Geophys. Res.*, 101, 3973–3988, 1996.

Gray, L. J., and J. A. Pyle, Two dimensional model studies of equatorial dynamics and tracer distributions, *Q. J. R. Meteorol. Soc.*, 113, 635–651, 1987.

Holton, J. R., and W. K. Choi, Transport circulation deduced from SAMS trace species data, *J. Atmos. Sci.*, 45, 1929–1939, 1988.

Jackman C. H., E. Fleming, S. Chandra, D. Considine, and J. Rosenfield, Past, present, and future modelled ozone trends with comparisons to observed trends, *J. Geophys. Res.* 101, 28753,-28767, 1996.

Jones, R. L., and J. A. Pyle, Observations of CH_4 and N_2O by the NIMBUS 7 SAMS: A comparison with in situ data and two dimensional numerical model calculations, *J. Geophys. Res.*, 89, 5263–5279, 1984.

Kumer, J. B., et al., Comparison of correlative data with nitric acid data version 7 from the CLAES instrument on UARS, *J. Geophys., Res.*, 101, 9621–9656, 1996.

McIntyre M. E., and T. N. Palmer, Breaking planetary waves in the stratosphere, *Nature*, 305, 593–600, 1983.

Mergenthaler, J. L., J. B. Kumer, and A. E. Roche, CLAES observations of the Mt. Pinatubo stratospheric aerosol, Geophys. Res., Lett., 22, 3497–3500, 1995.

Minschwaner, K., A. E. Dessler, J. W. Elkins, C. M. Volk, D. W. Fahey, M. Loewenstein, J. R. Podolske, A. E. Roche, and K. R. Chan, Bulk properties of isentropic mixing into the tropics in the lower stratosphere, *J. Geophys. Res.*, 101, 9433–9439, 1996.

Montzka. S. A., J. H. Butler, R. C. Myers, T. M. Thompson, T. H. Swanson, A. D. Clarke, L. T. Lock, and J. W. Elkins, Decline in the tropospheric abundance of halocarbons: Implications for stratospheric ozone depletion, Science, 272, 1318–1322, 1996.

Murcray, D. G., F. S. Bonomo, J. N. Brooks, A. Godlman, F. H. Murcray, and W. J. Williams, Detection of fluorocarbons in the stratosphere, *Geophys. Res. Lett.*, 2, 109–112, 1975.

Nightingale, R. W., et al., Global CF_2Cl_2 measurements by the UARS cryogenic limb array etalon spectrometer: Validation by correlative data and a model, *J. Geophys., Res.*,101, 9711–9736, 1996.

Park, J. H., Validation of Halogen Occultation Experiment CH_4 measurements from the UARS, *J. Geophys. Res.*, 101, 10183–10203, 1996.

Plumb, R. A., A "tropical pipe" model of stratospheric transport, *J. Geophys. Res.*, 101, 3957–3972, 1996.

Randel W. J., B. A. Boville, J. C. Gille, P. L. Bailey, S. T. Massie, J. B. Kumer, J. L. Mergenthaler, and A. E. Roche, Simulation of stratospheric N_2O in the NCAR CCM_2: Comparison with CLAES data and global budget analysis, *J. Atmos. Sci.*, 51, 2834–2845, 1994.

Randel, W. J., J. C. Gille, A. E. Roche, J. B. Kumer, J. L Mergenthaler, J. W. Waters, E. F. Fishbein and W. A. Lahoz, Stratospheric transport from the tropics to middle latitudes by planetary wave mixing, *Nature*, 365, 533–535, 1993.

Remedios, J. J., et al., Measurement of methane and nitrous oxide distributions by the improved stratospheric and mesospheric sounder: Retrieval and validation, *J. Geophys. Res.*, 101, 9843–9871, 1996.

Roche, A. E., et al., Validation of CH_4 and N_2O measurements by the CLAES instrument on the Upper Atmosphere Research Satellite, *J. Geophys. Res.*, 101, 9679–9710, 1996.

Roche, A. E., J. B. Kumer, J. L Mergenthaler, G. A. Ely, W. G. Uplinger, J. F. Potter, T. C. James, and L. W. Sterritt, The cryogenic limb array etalon spectrometer (CLAES) on the UARS: Experiment description and performance, *J. Geophys. Res.*, 98, 10763–10775, 1993.

Waugh, D. W., Seasonal variation of isentropic transport out of the tropical stratosphere, *J. Geophys Res.*, 101, 4007–4023, 1996.

WMO Report No. 37, *Scientific assessment of ozone depletion: 1994, World Meteorological Organization*, P.O. Box 2300, Geneva 2, CH 1211, Switzerland, 1995.

Zander R., et al., The 1994 northern midlatitude budget of stratospheric chlorine derived from ATMOS observations from space, *Geophys. Res. Lett.*, 23, 2357–2360, 1996.

Volk, C. M., Quantifying transport between the tropical and mid-latitude lower stratosphere, *Science*, 272, 1763–1768, 1996.